

Supporting Information

Materials and Methods

Patterned substrate of fluid ephrinA1 and immobilized RGD

Phospholipid vesicles were prepared using previously published methods (1). Two kinds of lipids mixtures were used in this study, 96% of DOPC (1,2-dioleoyl-sn-glycero-3-phosphocholine) plus 4% of Ni-NTA-DOGS (1,2-dioleoyl-sn-glycero-3-[(N-(5-amino-1-carboxypentyl)iminodiacetic acid)-succinyl]), or 99% of DOPC plus 1% of Marina Blue-DHPE (Marina Blue-1,2-dihexadecanoyl-sn-glycero-3-phosphoethanolamine) (Avanti lipids). To prepare patterned substrate of SLB and immobilized polymer, clean coverslips were incubated with PLL-g-PEG-biotin (50%, Susos) for at least two hours. The coated coverslips were then etched by deep UV with a designed photomask to generate patterns. Lipid vesicles were then deposited on the coverslips to form SLB on the etched surface only. The patterns were regular arrays of circles with diameter of $D = 1$ to $4 \mu\text{m}$, and centre to centre distance of $3 \times D$. The three components substrates including SLB, PLL-g-PEG-biotin and PLL-g-PEG were made by two steps UV etch. After the first etch on PLL-g-PEG-biotin surface, the coverslip was then coated with PLL-g-PEG, and underwent another etch to form SLB. The two etch processes were aligned under microscope to achieve a desired layout of the three components.

After SLB formation, the substrates were blocked by 0.05% bovine serum albumin (BSA; Sigma-Aldrich) for 2 hours, and then incubated with $1 \mu\text{g/ml}$ of DyLight-405 NeutrAvidin (Thermo-Fisher) for 30 minutes to bind biotin. After rinse, the substrates were then incubated with a solution of 5nM of ephrinA1-Alexa 680 and $1 \mu\text{g/ml}$ of RGD-PEG-PEG-biotin (Peptides international) for 60 min for surface functionalization. EphrinA1 was expressed with a C-terminal 10-histidine tag and purified from insect cell culture (2), and labelled with Alexa 680 fluorophore (Thermo-Fisher) followed by vender's manual. EphrinA1 density on SLB was calibrated with quantitative fluorescence microscopy (3). The protein incubation solutions were then exchanged with imaging buffer (25 mM Tris, 140 mM NaCl, 3 mM KCl, 2 mM CaCl_2 , 1 mM MgCl_2 , and 5.5 mM D-glucose) and warmed up to 37°C prior addition of cells.

Cell culture, plasmid and preparation for live cell experiments

MDAMB231 cells (ATCC) were grown in DMEM (high glucose) (Thermo-Fisher) supplemented with 10% fetal bovine serum (FBS) (Thermo-Fisher) and 1% penicillin/streptomycin (Thermo-Fisher), at 37°C and in an atmosphere of 5% CO_2 . MCF10A cells (Ronen Zaidel Bar's group) were cultured in DMEM/F12 (Thermo-Fisher) supplemented with 5% horse serum (Thermo-Fisher), 20 ng/ml EGF (Sigma), 0.5 mg/ml hydrocortisone (Sigma), 100 ng/ml cholera toxin (Sigma), $19 \mu\text{g/ml}$ insulin (Sigma), and 1% penicillin/streptomycin. PC3 cells (ATCC) were grown in RPMI 1640 supplemented with 10% FBS and 1% penicillin/streptomycin.

MDAMB231 cells were transfected by Lipofectamine 2000 (Thermo-Fisher). Paxillin-EGFP (4), cSrc-GFP (5), and Myosin light chain-GFP (6) plasmids are generous gifts from Dr. Michael Sheetz's lab (Mechanobiology Institute). Src-SH2-tdEOS and Grb2-tdEOS (7) are generous gifts from Dr. Ji Yu's lab (University of Connecticut Health Center). Src-EOS3.2 (8) is a generous gift from Dr. Michael Davidson (maintained by Dr. Pakorn Kanchanawong, Mechanobiology Institute). Arp3-mcherry (9) is a generous gift from Dr. Alexandra Bershadsky's lab (Mechanobiology Institute). Before experiments, cells were detached by PBS based dissociation buffer (Thermo-Fisher) for 5 min at 37 °C, and resuspended in the imaging buffer. The cells were then added into pre-warmed cell chambers to interact with the substrates.

Immunostaining and western blotting

Following 0.5-2h of incubation on the substrates, cells were fixed with 4% paraformaldehyde, and permeabilized with 0.1% Triton-X with standard immunostaining protocol. Primary antibodies include rabbit anti EphA2 (CST, 7997S), rabbit anti pY588-EphA2 (CST, 12677S) , mouse anti paxillin (BD Biosciences, 610052), rabbit anti pY118-paxillin (Thermo-Fisher, 44-722G), mouse anti FAK (Abcam, ab105917), rabbit anti pY576-FAK (Thermo-Fisher, 700013), Alexa 488 labelled phalloidin (Thermo-Fisher A12379), rabbit anti pY700-Cbl (Abcam, ab76002), rabbit anti pS19-myosin light chain (CST, 3671), and rabbit anti pY419-Src (CST, 2101S). Secondary antibodies include goat anti rabbit or goat anti mouse antibodies conjugated with Alexa fluorophores (Alexa 488, Alexa 568, Alexa 594, Alexa 647, Thermo-Fisher). Western blotting of EphA2, FAK and paxillin phosphorylation was done after 1 hour incubation of cells with different substrates. Cells were lysed in buffer containing phosphatase and protease inhibitors (Sigma), followed with standard western blot protocol.

Cell imaging

An Eclipse Ti inverted microscope (Nikon) with a TIRF system and Evolve EMCCD camera (Photometrics) was used for most cell imaging. TIRF microscopy was performed with a 100x TIRF objective with a numerical aperture of 1.49 (Nikon) and an iChrome MLE-L multilaser engine as a laser source (Toptica Photonics). The localized photoactivation experiment and other imaging were performed in an Eclipse Ti inverted microscope (Nikon) with CSU-X1 confocal spinning disk unit (Yokogawa), controlled with iLAS and Metamorph software (Molecular Devices).

Time-lapse single molecule imaging of Src-mEOS3.2 was performed in TIRF microscopy, in a way such as to optimize signal-to-noise and temporal resolution by coupling minimizing laser power and maximizing video rate. To increase tracking accuracy, the density of individual Src-mEOS3.2 molecules was controlled by 405 nm laser illumination to be about $\sim 0.05 / \mu\text{m}^2$. In cells co-transfected with paxillin-GFP and Src-mEOS3.2, spreading on Alexa 680 labelled ephrinA1 substrate, green channel (ex=488 nm, em = 525 (50) nm) and far-red channel (ex =647 nm, em > 655 nm) were acquired before single molecule recording to localize FAs and ephrinA1 clusters. Both FAs and ephrinA1 clusters move significantly slower compared to

individual Src-mEOS3.2 molecules. The autofluorescence on the red channel was completely photobleached before photoactivating mEOS3.2 by a 405 nm beam for 200 ms. After photoactivation, a small amount of Src-mEOS3.2 molecules were visualized and recorded by EMCCD with 10 - 40 fps video rate. Each movie contains 1000 frames for further analysis.

Image analysis

Paxillin immunofluorescence images were background subtracted and thresholded to locate every single FA for morphologic measurement. In parallel, the cell shape was masked by actin fluorescent images to generate a distance map which represents the distance of every pixel to its nearest cell boundary. The two analyzed images were combined to calculate the distance of every FA to its nearest cell boundary. All processes were automated with a home-written ImageJ Macro.

For live cell paxillin-GFP tracking, a cross-correlation single particle tracking method was used to determine the centroid positions of paxillin-GFP clusters (10, 11). A FA trajectory was created by connecting the subsequent xy coordinates through the frames using the nearest neighbor method. All trajectories of FAs were used to create a lifetime map by a home-written Matlab program. The lifetime distribution was fitted with second order exponential decay function $y=y_0+A_1e^{-t/\tau_1}+A_2e^{-t/\tau_2}$, and normalized by the highest probability, providing two characteristic time constants, fast constant τ_1 and slow constant τ_2 . However we used the slower characteristic time constant (τ_2) in comparison of different samples due to no significant difference in the fast characteristic time constant (τ_1). The number of newly created paxillin-GFP clusters every frame was used to determine FA formation rate as a function of cell spreading time. The rate fluctuated along the time, but average value was used to compare from sample to sample. Similar methods were applied in Src-SH2-tdEOS tracking.

The same above algorithm was applied for tracking Src-mEOS3.2 single molecules. We chose trajectories outside of both FAs and ephrinA1 clusters to measure Src-mEOS3.2 membrane diffusion. Using several thousands of trajectories over 10 frame lengths, we calculated MSD at time-lag ($dt = 0.05$ sec) for each trajectory. The mean MSD- dt curve was obtained and showed free diffusion behavior up to a time scale of 1 sec (Figure S6B). The MSD- dt curve was fitted with normal diffusion equation ($\langle r^2 \rangle = 4Dt$), providing the diffusion coefficient of $D = 0.38 \mu\text{m}^2/\text{s}$. The distribution of individual D values derived from individual MSD- dt curves has a peak value at $D = 0.41 \pm 0.015 \mu\text{m}^2/\text{s}$ (Figure S6C), similar as mean MSD- dt fitting result.

To search for Src single molecule translocation trajectories from ephrinA1 clusters to FAs, EphrinA1 and FA images were first thresholded to generate masks. The translocation trajectory was defined as that Src-mEOS3.2 must first appear in ephrinA1 cluster region, diffuse out, and finally bind FAs. Src-mEOS3.2 binding to ephrinA1 clusters and FAs was further defined such that the distance (d) between any two consecutive xy coordinates within an ephrinA1 cluster or a FA region is smaller than the distance (d') that a Src molecule travels by free diffusion on the membrane (12, 13). Given $D = 0.41 \mu\text{m}^2/\text{s}$, d' is calculated as 286 nm for 0.05 s. A total of 3,916 Src trajectories were analyzed. 2,837 trajectories remain

in ephrinA1 cluster region, 967 diffuse out, and 62 bind nearby FAs.

References

1. Lin W-C, Yu C-H, Triffo S, & Groves JT (2009) Supported Membrane Formation, Characterization, Functionalization, and Patterning for Application in Biological Science and Technology. *Current Protocols in Chemical Biology*, (John Wiley & Sons, Inc.).
2. Greene Adrienne C, *et al.* (2014) Spatial Organization of EphA2 at the Cell-Cell Interface Modulates Trans-Endocytosis of EphrinA1. *Biophysical Journal* 106(10):2196-2205.
3. Galush WJ, Nye JA, & Groves JT (2008) Quantitative fluorescence microscopy using supported lipid bilayer standards. *Biophysical Journal* 95(5):2512-2519.
4. Sathe AR, Shivashankar GV, & Sheetz MP (2016) Nuclear transport of paxillin depends on focal adhesion dynamics and FAT domains. *Journal of Cell Science* 129(10):1981-1988.
5. Shvartsman DE, *et al.* (2007) Src kinase activity and SH2 domain regulate the dynamics of Src association with lipid and protein targets. *J Cell Biol* 178(4):675-686.
6. Giannone G, *et al.* (2004) Periodic Lamellipodial Contractions Correlate with Rearward Actin Waves. *Cell* 116(3):431-443.
7. Oh D, *et al.* (2012) Fast rebinding increases dwell time of Src homology 2 (SH2)-containing proteins near the plasma membrane. *Proceedings of the National Academy of Sciences* 109(35):14024-14029.
8. McKinney SA, Murphy CS, Hazelwood KL, Davidson MW, & Looger LL (2009) A bright and photostable photoconvertible fluorescent protein. *Nat Meth* 6(2):131-133.
9. Taylor MJ, Perrais D, & Merrifield CJ (2011) A high precision survey of the molecular dynamics of mammalian clathrin-mediated endocytosis. *PLoS Biol* 9(3):e1000604.
10. Gelles J, Schnapp BJ, & Sheetz MP (1988) Tracking kinesin-driven movements with nanometre-scale precision. *Nature* 331(6155):450-453.
11. Oh D, Yu Y, Lee H, Wanner Barry L, & Ritchie K (2014) Dynamics of the Serine Chemoreceptor in the Escherichia coli Inner Membrane: A High-Speed Single-Molecule Tracking Study. *Biophysical Journal* 106(1):145-153.
12. Shimrat M (1962) Algorithm 112: Position of point relative to polygon. *Commun. ACM* 5(8):434.
13. Hormann K & Agathos A (2001) The point in polygon problem for arbitrary polygons. *Computational Geometry* 20(3):131-144.

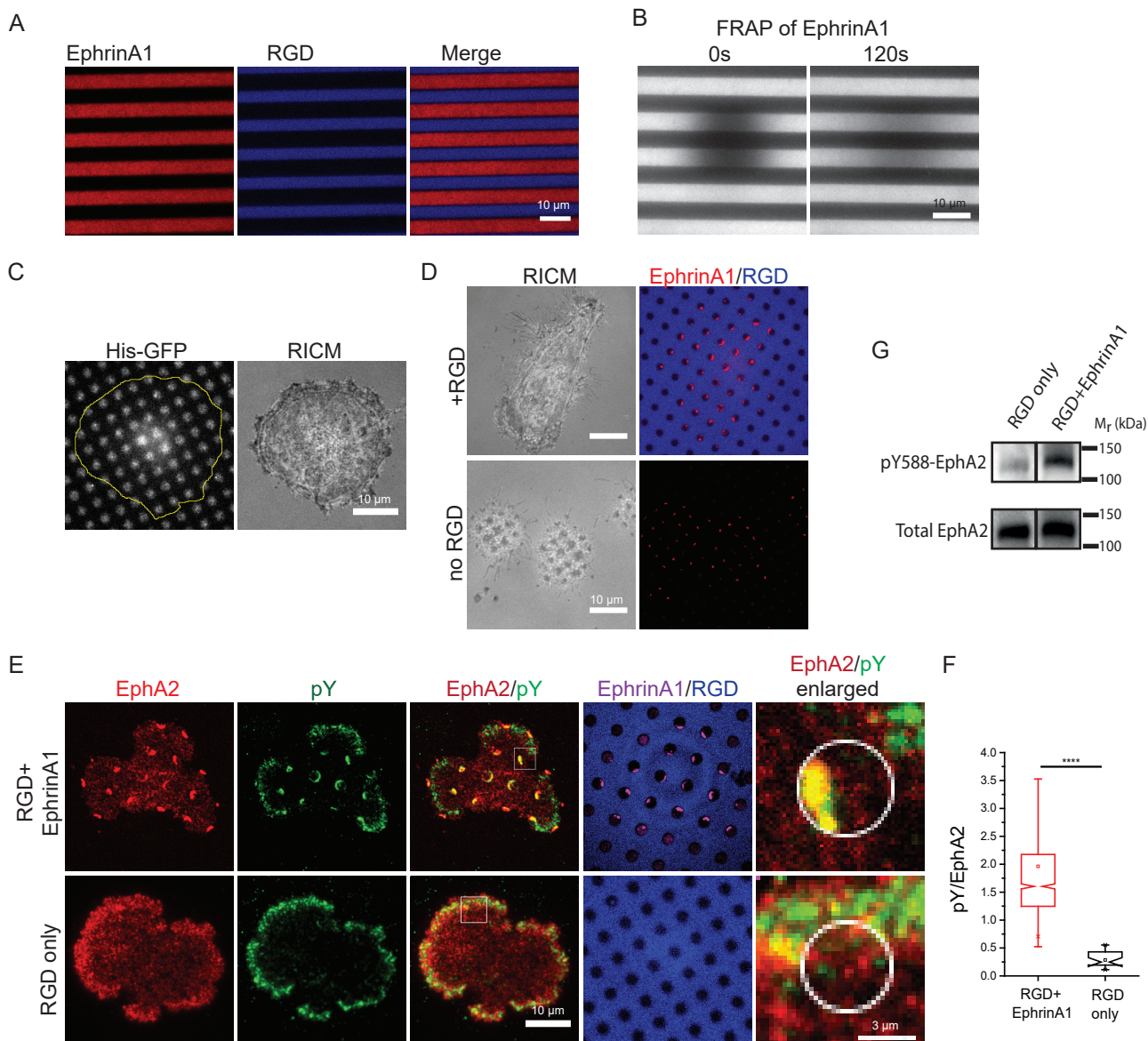


Figure S1. Spatially controlled activation of EphA2 and integrin on a micropatterned hybrid substrate of fluid ephrinA1 and immobilized RGD.

(A and B) Diffusion of ephrinA1 on the SLB region shown by fluorescence recovery after photobleaching (FRAP) in a stripe pattern.

(C) Cell spread on the substrate of fluid GFP and immobilized RGD.

(D) Comparison of cells spread on the hybrid substrate with or without RGD.

(E and F) (E) Immunostaining fluorescence images of cells fixed after 1 hour spreading on indicated substrates. The rightmost column is enlarged images from selected ROIs marked by white box. The integral intensities of EphA2 and pY were measured in each white circular region and their ratio is plotted in (F). N=1045 circles were quantified from 50 cells in RGD+EphrinA1 samples, and N=206 circles were quantified from 10 cells in RGD control samples.

(G) Western blot of pY588-EphA2 and total EphA2 of cells lysed after 1 hour interaction with indicated substrates.

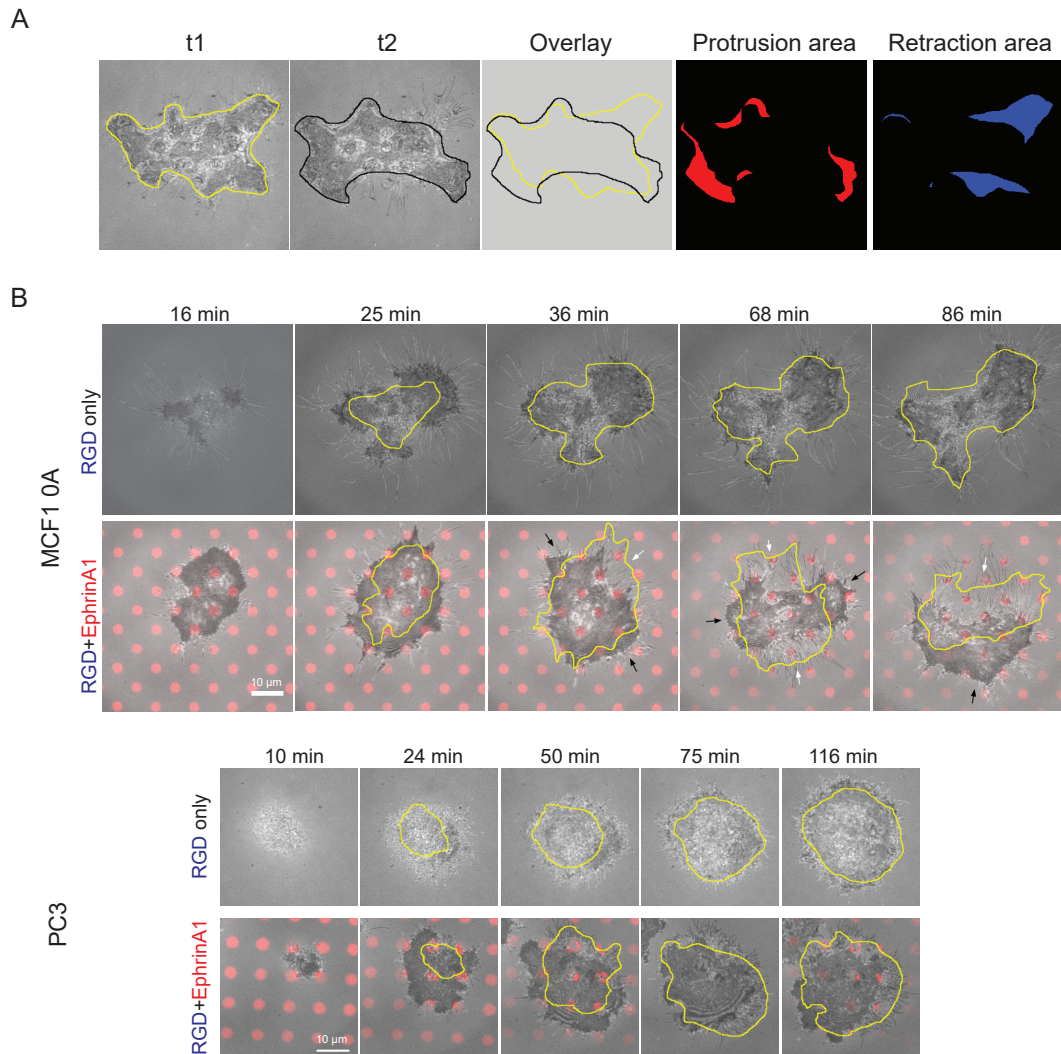


Figure S2. EphA2 activation changes cell spreading behavior by inducing local retractions and protrusions.

(A) Illustration of method used to calculate protruded and retracted area.

(B) Time-course images of MCF10A and PC3 cells spreading either on RGD only or RGD+EphrinA1 substrates. Conditions are same as Figure 2(A).

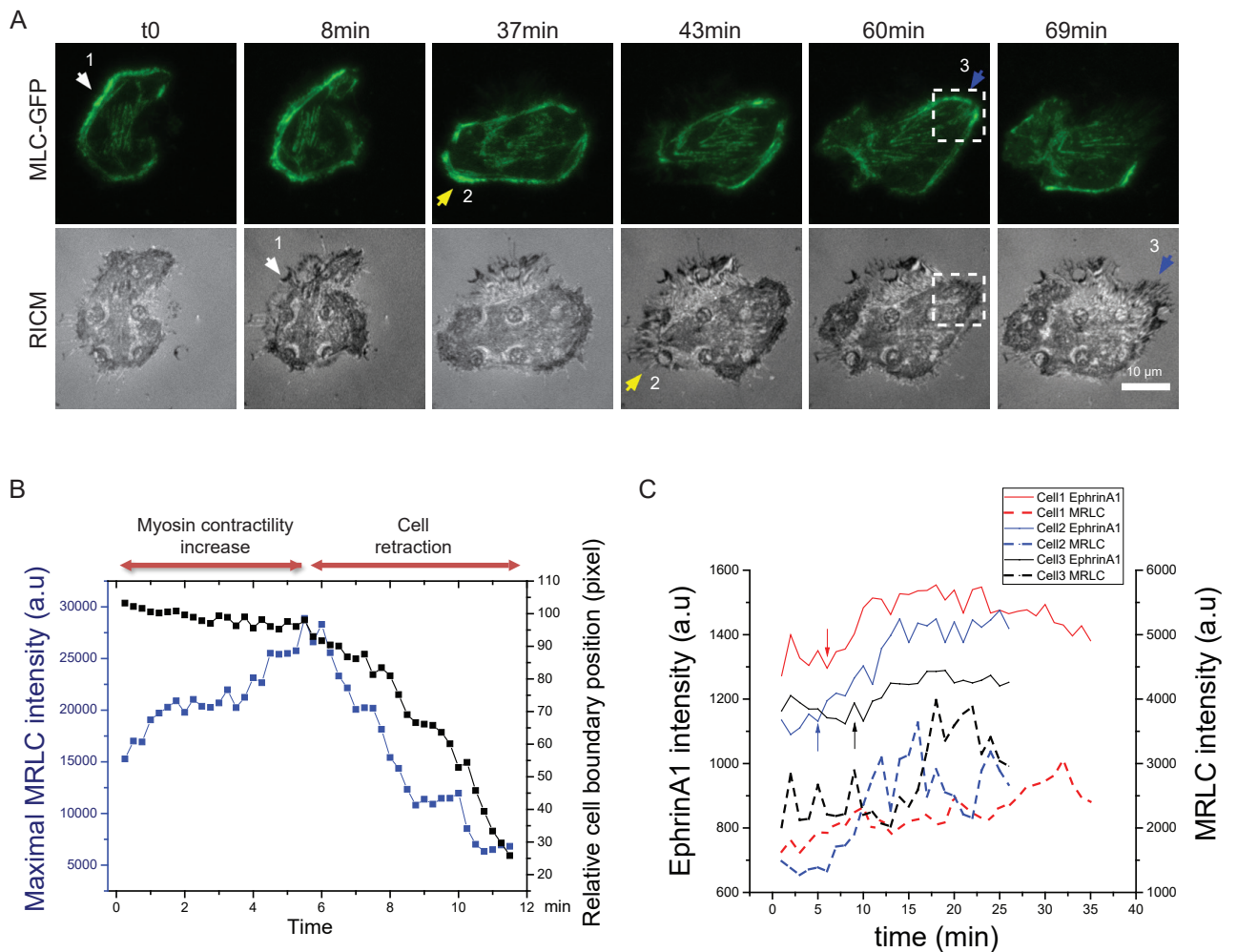


Figure S3. EphA2 induced local retraction is dependent on myosin II activation.

(A) Time-course images of a MLC-GFP transiently transfected cell spreading on EphrinA1+RGD substrate. White, yellow and blue arrows indicate three events of MLC-GFP accumulation (upper panel) and subsequent retraction (lower panel).
 (B) Time-course graph of maximal MLC-GFP intensity and relative cell boundary position in a selected ROI in panel A (white dashed line box). The relative cell boundary position is measured by the length between cell edge and lower left corner of the ROI box.
 (C) Time-course fluorescence intensities of a single ephrinA1 cluster and nearby MRLC-GFP in N=3 cells in conditions similar with Figure 3(C-E). Arrows indicate start of ephrinA1 clustering.

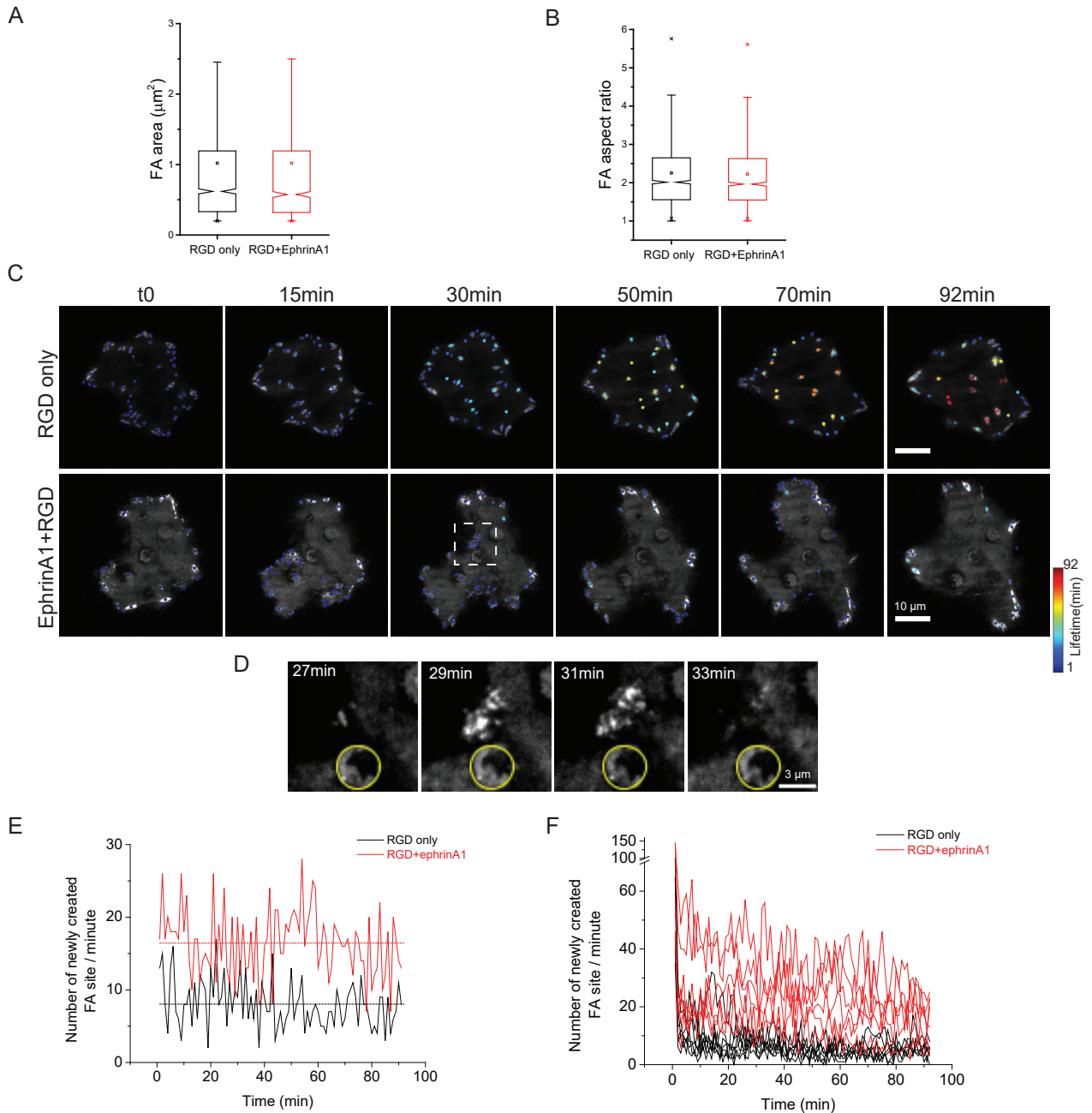


Figure S4. EphA2 signaling increases FA dynamics.

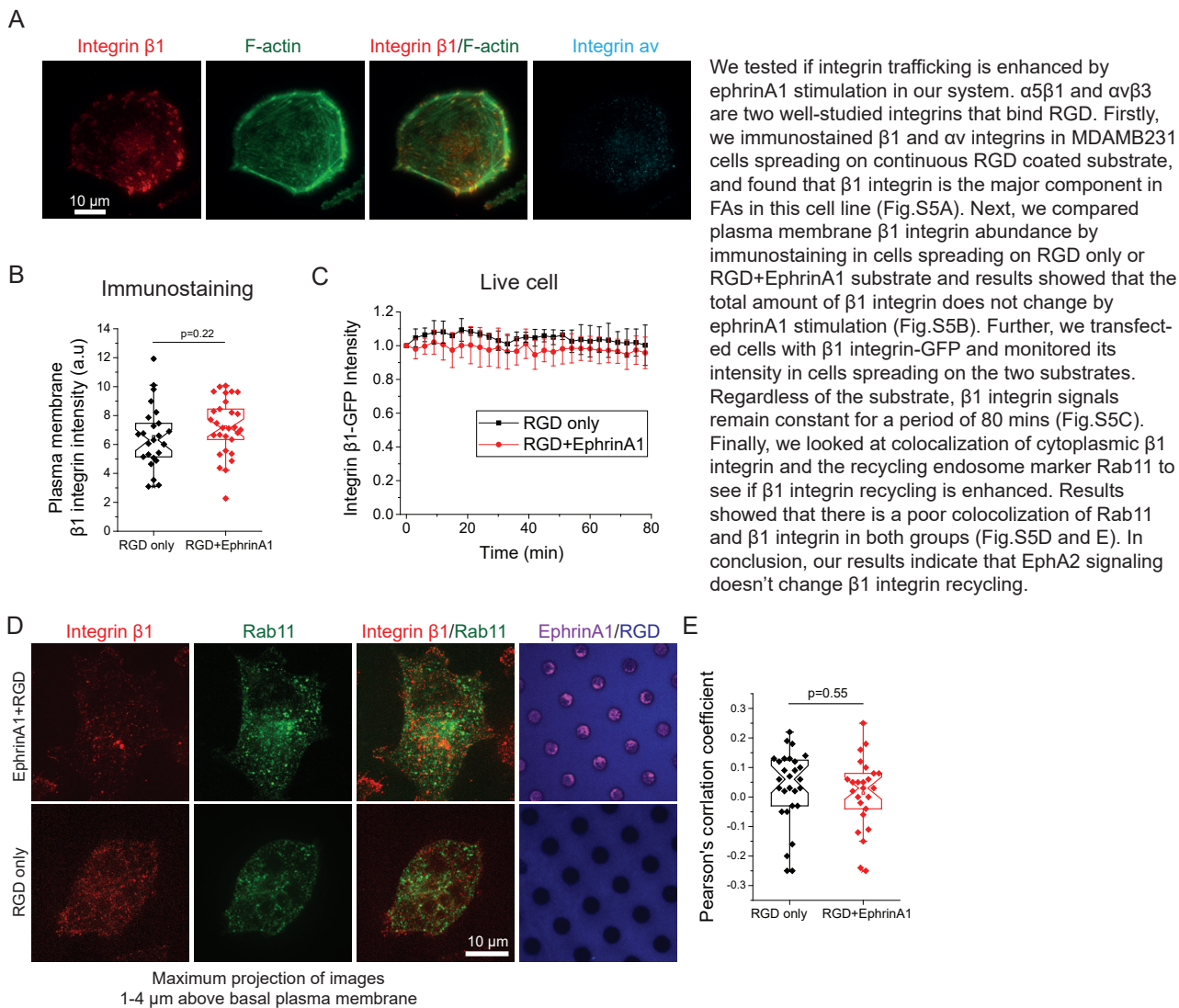
(A-B) Quantifications of FAs (A) area and (B) aspect ratio. Conditions are same as Figures 4(A-C).

(C) Time-course, lifetime color coded images of paxillin-GFP expressing cells spreading on indicated substrates. Conditions are same as Figure 4D.

(D) Zoom-in images from a selected ROI in panel C (white dashed line box), with a yellow circle to mark a SLB region.

(E) Time-course FA formation rate graph of cells shown in panel C.

(F) Time-course FA formation rate graph of a group of cells. N=7 for RGD only substrate, and N=6 for RGD+EphrinA1 substrate.



We tested if integrin trafficking is enhanced by ephrinA1 stimulation in our system. $\alpha 5\beta 1$ and $\alpha v\beta 3$ are two well-studied integrins that bind RGD. Firstly, we immunostained $\beta 1$ and αv integrins in MDAMB231 cells spreading on continuous RGD coated substrate, and found that $\beta 1$ integrin is the major component in FAs in this cell line (Fig.S5A). Next, we compared plasma membrane $\beta 1$ integrin abundance by immunostaining in cells spreading on RGD only or RGD+EphrinA1 substrate and results showed that the total amount of $\beta 1$ integrin does not change by ephrinA1 stimulation (Fig.S5B). Further, we transfected cells with $\beta 1$ integrin-GFP and monitored its intensity in cells spreading on the two substrates. Regardless of the substrate, $\beta 1$ integrin signals remain constant for a period of 80 mins (Fig.S5C). Finally, we looked at colocalization of cytoplasmic $\beta 1$ integrin and the recycling endosome marker Rab11 to see if $\beta 1$ integrin recycling is enhanced. Results showed that there is a poor colocalization of Rab11 and $\beta 1$ integrin in both groups (Fig.S5D and E). In conclusion, our results indicate that EphA2 signaling doesn't change $\beta 1$ integrin recycling.

Figure S5. EphA2 induced FA dynamics is not dependent on integrin trafficking.

- (A) Immunostaining fluorescence images of cells fixed after 1.5h of spreading on RGD substrate.
- (B) Quantification of $\beta 1$ integrin intensity on plasma membrane in cells fixed after 1.5h of spreading on different substrates.
- (C) Monitoring of $\beta 1$ integrin-GFP transfected cells spreading on different substrates. N=3 for both groups. Data are presented as mean \pm S.D.
- (D) MDAMB231 cells were transfected with Rab11-GFP, spread on RGD only or RGD+EphrinA1 substrates for 1.5h, and immunostained with $\beta 1$ integrin. Confocal images were acquired from 1 μm above basal plasma membrane until 4 μm into cells. Stack images of Rab11 and $\beta 1$ integrin were projected by maximum intensity and were used for Pearson's correlation analysis in (E).

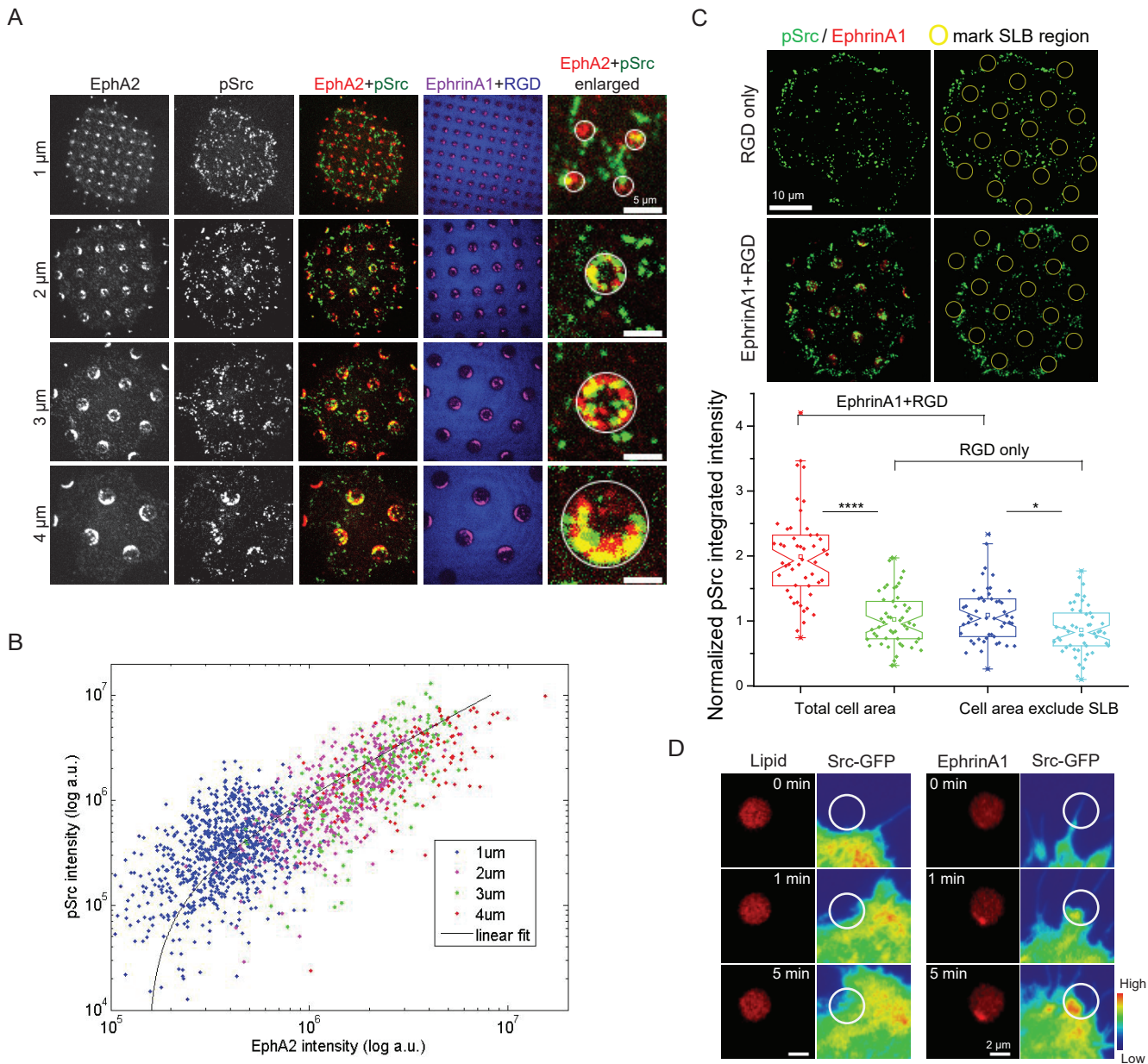


Figure S6. Src kinase is recruited and activated in EphA2 clusters.

(A-B) Linear correlation between EphA2 receptor and pSrc. (A) Immunostaining fluorescence images of pY416-Src and EphA2 of cells fixed after 1 hour of spreading on indicated substrates. The substrates have different circular SLB corrals with diameters of $D=1, 2, 3,$ and $4 \mu\text{m}$ and center to center distance of $3xD$. The integral intensities of EphA2 and pSrc were measured in each SLB region, and pSrc versus EphA2 intensity are plotted in (B). Data points from different samples are marked with different colors, and fitted with linear correlation equation. Pearson's correlation coefficient $r=0.74$.

(C) Quantification of pSrc intensity in total cell area and cell area excluding SLB regions. Total cell pSrc intensity is almost doubled in the presence of ephrinA1. After erase of pSrc signals in SLB regions both in RGD only and EphrinA1+RGD samples, EphrinA1+RGD group still has about 15% higher pSrc intensity compared with RGD only group. $N=50$ for both RGD and RGD+EphrinA1 groups. Significance was tested by student's t test.

(D) Typical time-course live cell images of cSrc-GFP and ephrinA1 during cell spreading in a cell edge area where only one patch of SLB is shown. For control, SLB is marked by 1% Marina Blue DHPE. Src-GFP images are pseudo-color coded to highlight intensity difference.

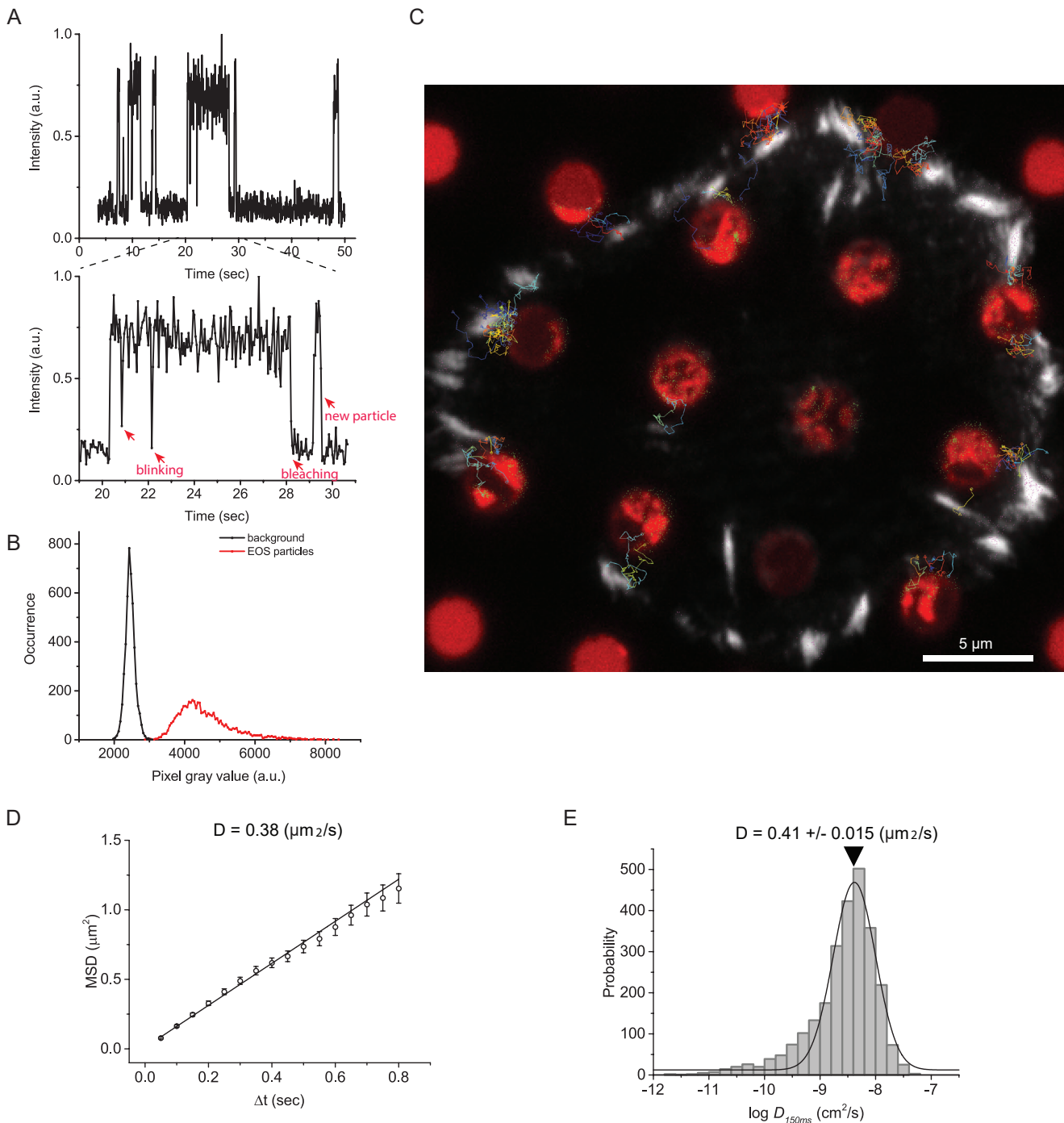


Figure S7. Src single molecule diffusion.

(A) Single step photobleach of Src-mEOS3.2 in live cells.

(B) Distribution of Src-mEOS3.2 fluorophore intensities in a live cell movie.

(C) Full cell high resolution image of Figure 5G.

(D-E) Diffusion coefficient of Src-mEOS3.2 on plasma membrane measured by (D) Mean square displacement curve, providing $D = 0.38 \text{ } \mu\text{m}^2/\text{s}$ and (E) individual diffusion coefficient distribution. The diffusion coefficient distribution is fitted with Gaussian function, providing peak value at $D = 0.41 \pm 0.015 \text{ } \mu\text{m}^2/\text{s}$.

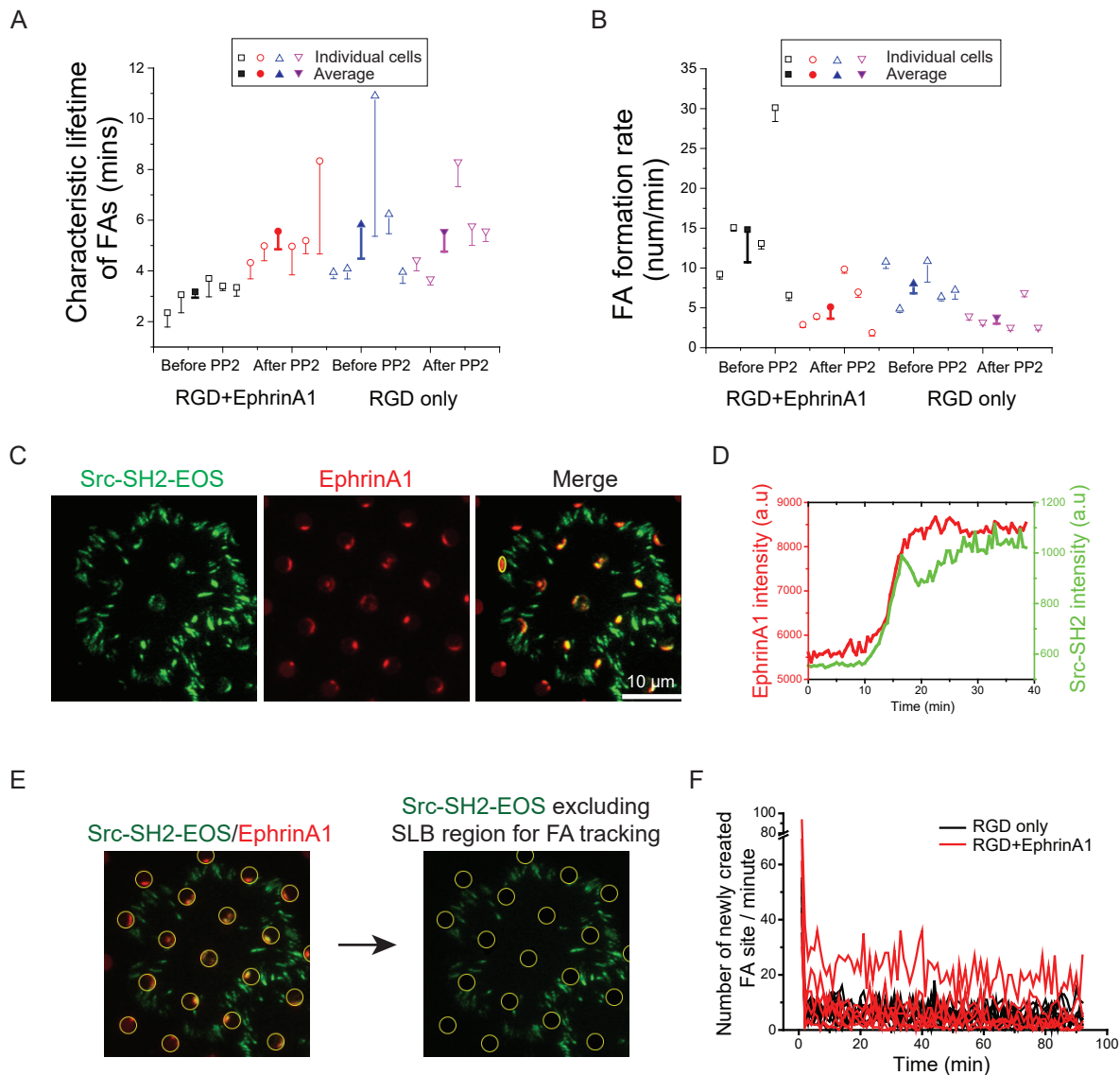


Figure S8. EphA2 induced FA dynamics increase is dependent on Src.

(A) Quantification of FA characteristic lifetime and (B) FA formation rate before and after PP2 treatment on indicated substrates. (C) Live cell fluorescence images of a Src-SH2-tdEOS transiently expressed cell spreading on RGD+EphrinA1 substrate. (D) A typical time-course fluorescence intensity track of Src-SH2-tdEOS and ephrinA1 from a selected ROI of panel A (yellow circle) during cell spreading. (E) Illustration of method used to track Src-SH2-tdEOS to reflect FAs. (F) Time-course FA formation rate graph of a group of Src-SH2-tdEOS overexpressing cells.

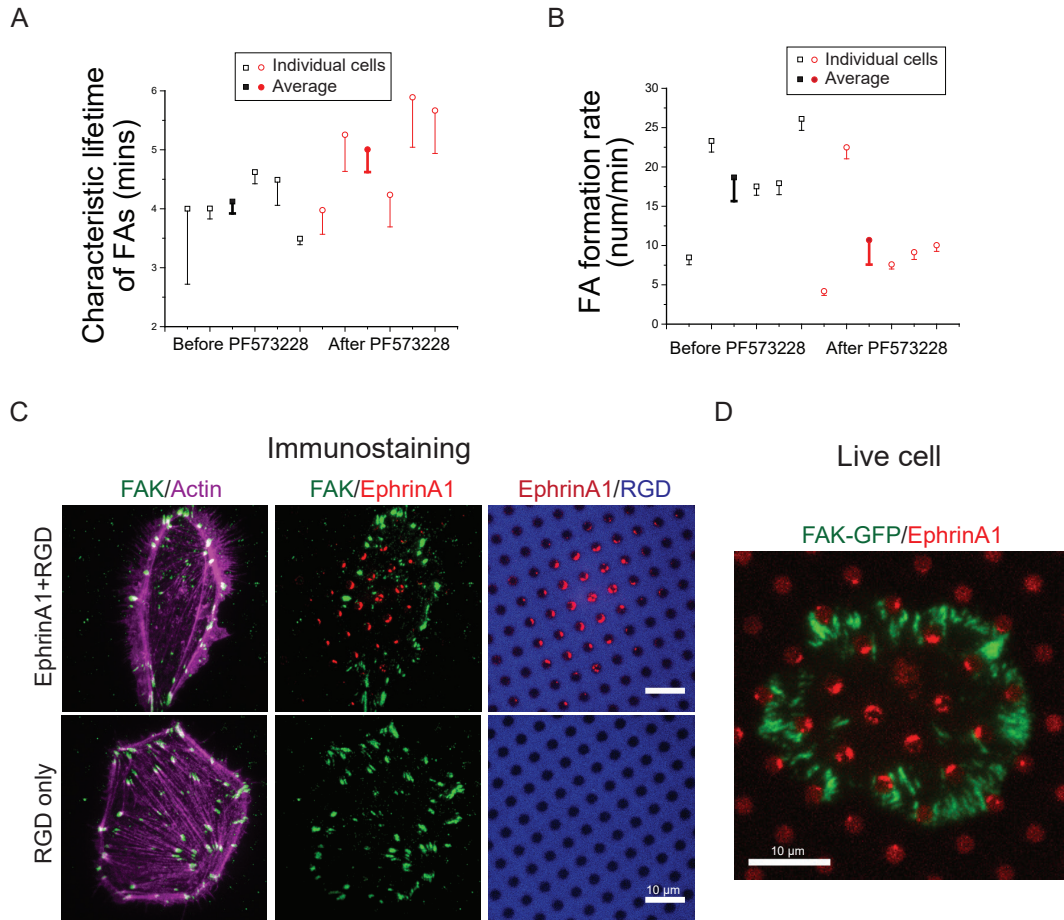


Figure S9. EphA2 induced FA dynamics increase correlates with FAK phosphorylation.

(A) Quantification of FA characteristic lifetime and (B) FA formation rate before and after PF573228 treatment on RGD+EphrinA1 substrate.

(C) Immunostaining fluorescence images of cells fixed after 1.5h of spreading on different substrates and (D) FAK-GFP transfected cells spread on RGD+EphrinA1 substrate.

Supplimentary movies

Movie1 Formation of ephrinA1:EphA2 signaling clusters in spreading cells.

Movie2 EphrinA1 changes cell spreading behavior by inducing local retractions and protrusions in MDA-MB-231 cell.

Movie3 EphrinA1 changes cell spreading behavior by inducing local retractions and protrusions in MCF10A and PC3 cells.

Movie4 MLC-GFP dynamics in cells spreading on the hybrid substrate.

Movie5 Localized MLC-GFP dynamics in response to ephrinA1 stimulation.

Movie6 EphA2 activation increases focal adhesion dynamics throughout the cell.

Movie7 Src single molecule translocation from ephrinA1:EphA2 clusters to FAs by membrane diffusion.

Movie8 Paxillin-GFP dynamics before and after Src inhibition in cells spreading on the hybrid substrate.

Movie9 Src-SH2-tdEOS dynamics in cells spreading on the hybrid substrate.

Movie10 Paxillin-GFP dynamics before and after FAK inhibition in cells spreading on the hybrid substrate.

Movie11 Polarized presentation of ephrinA1 induces directed cell migration.